

Comparison Between two Single-Switch Isolated Flyback and Forward High-Quality Rectifiers for Low Power Applications

G. Spiazzi, S. Buso

Department of Electronics and Informatics - University of Padova

Via Gradenigo 6/a, 35131 Padova - ITALY

Phone: +39-049-827.7525 Fax: +39-049-827.7699

e-mail: giorgio.spiazzi@dei.unipd.it, simone.buso@dei.unipd.it

Abstract - In this paper, two isolated single-switch high-quality rectifiers are compared: one is based on the forward topology with secondary side resonant reset, the other is a flyback rectifier with a lossless passive snubber. These rectifiers were both designed for universal input voltage range ($90 + 260 V_{RMS}$) and 200 W nominal output power. The adopted control technique is a modified non-linear carrier control based on the integration of the switch current signal, which does not require any input voltage sensing, analog multiplier and current error amplifier. The comparison is based both on theoretical analysis and measurements on fully developed prototypes and takes into account the following aspects: basic design guidelines, voltage and current rating of active devices, power losses on the main devices, overall efficiency and conducted EMI generation. This work, highlighting advantages and drawbacks of both the selected topologies, will allow designers to make a proper choice for a given application in the low power range (below 300W).

I. INTRODUCTION

The field of power factor correctors (PFC's), i.e. rectifiers that draw a current from the line proportional to the input voltage (unity power factor), is almost totally dominated by the boost topology, especially for medium to high power applications. A two stage approach is normally employed where the required isolation is provided by a second dc/dc stage. For low power applications (below 300 W), flyback and forward topologies become more attractive, since they provide both isolation and overcurrent protection in just one conversion stage. However, the flyback topology requires the designer to take care of the non negligible transformer leakage inductance, while the forward topology is limited by its inability to draw current from the line when the input voltage is lower than the reflected output voltage.

In this paper a forward rectifier with secondary side resonant reset [1] and a flyback rectifier with a lossless passive snubber [2] are compared in order to fully highlight advantages and drawbacks of both topologies. The same control technique was adopted, i.e. the modified non linear carrier control described in [2-4], which does not require input voltage sensing and current error amplifier.

The analysis and suggested design procedure for both topologies are already reported in [1] and [2] respectively, therefore this paper will focus on the following aspects, not covered in the mentioned papers:

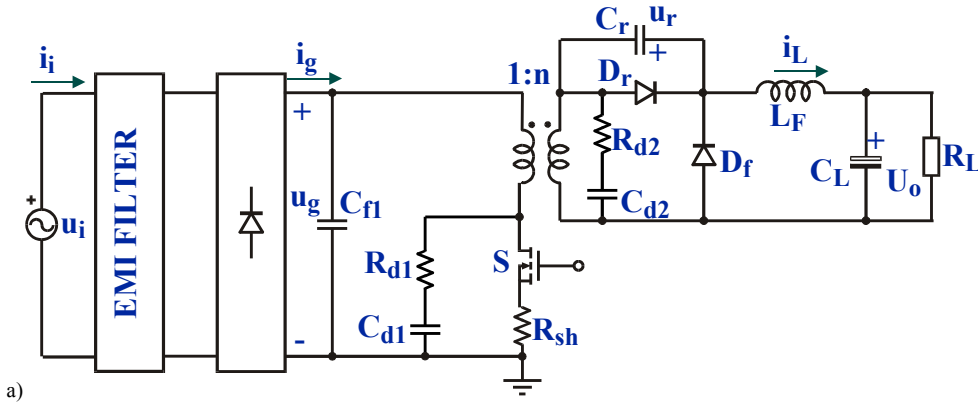
- voltage and current ratings of the main devices for universal input voltage range (from 90 to $260 V_{RMS}$);
- power dissipation of main active devices;
- overall efficiency at variable input voltage and load;
- conducted electromagnetic noise generation.

The comparison is based both on theoretical analysis and measurements on fully developed prototypes, both rated for 200 W, at 48 V output voltage, and for universal input voltage range.

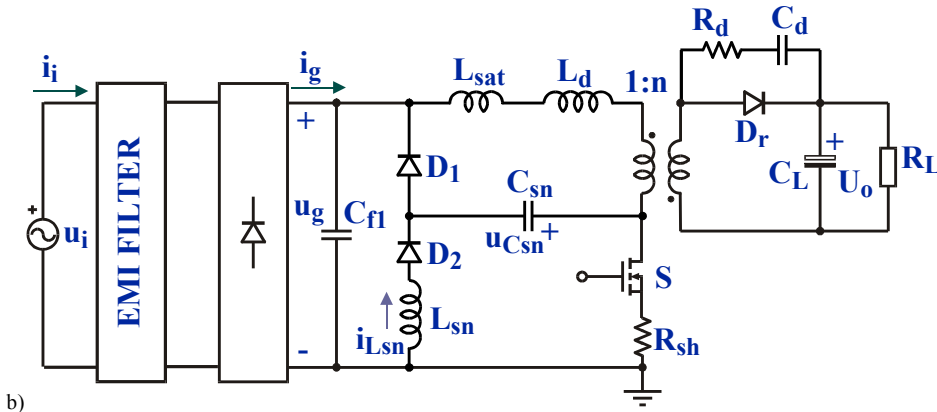
II. CONVERTER DESCRIPTION

The forward rectifier with secondary side resonant reset is shown in Fig. 1a. As described in [1], the secondary-side resonant reset scheme is simply made up of capacitor C_r connected in parallel with the rectifier diode D_r . The transformer reset occurs through the resonance between its magnetizing inductance L_m and the resonant capacitor C_r during the switch off-time and the mechanism is conceptually equal to the standard resonant reset scheme, which exploits the switch output capacitance C_{DS} . The only difference is that the transformer stored energy can now be partially delivered to the load instead of being dissipated in the switch at turn on. This behavior gives the step-up capability needed to draw current from the line during the whole line period. Since the needed magnetizing inductance value requires a small air gap in the transformer, the increased leakage inductance calls for suitable snubbers both at the primary and the secondary side (R_d - C_d networks in Fig. 1a).

The scheme of the flyback rectifier with a lossless passive snubber is reported in Fig. 1b. As described in [2], the snubber capacitor C_{sn} controls the switch dv/dt at turn-off and recovers the leakage inductance energy to the input capacitor C_{fl} , through inductor L_{sn} and diodes D_1 and D_2 . A passive snubber R_d - C_d across the rectifier diode D_r takes care of the secondary side leakage inductance, while the small saturable



CONVERTER COMPONENTS	
S	IRG4PF50
D _r , D _f	RURP1560
L _F	MPP55254
Transformer	E 42-21-20



CONVERTER COMPONENTS	
S	IRG4PF50
D _r	RURG3060
D ₁ , D ₂	RURP8120
Saturable reactor	A _L = 5110 nH, T38
L _{sn}	Kool-Mμ 77930-A7
Transformer	Kool-Mμ 77438-A7

Fig. 1 – a) Forward rectifier with secondary-side resonant reset. b) Flyback rectifier with lossless passive snubber.

reactor L_{sat} damps parasitic oscillations occurring at D_1 's turn-off.

III. VOLTAGE AND CURRENT RATINGS

The basic converter specifications are given in Table I. The two converters can be designed following the procedures outlined in [1] and [2], whose critical aspects are summarized in the following.

TABLE I
RECTIFIER SPECIFICATIONS

Nominal output power	P_o	200	[W]
Nominal output voltage	U_o	48	[V]
Nominal input voltage	U_i	90 ÷ 260	[V _{RMS}]
Switching frequency	f_s	56	[kHz]

A. Flyback rectifier

Even if the presence of the lossless snubber slightly alters the voltage conversion ratio of the flyback converter [2], the standard relation of the flyback topology can still be used to design the power converter. The transformer turns ratio is a critical parameter determining the voltage stress on the switch and the achievement of soft-switching. The design of the

lossless snubber requires the choice of the snubber capacitor and inductor values as well as the selection of the auxiliary diodes D_1 and D_2 . As far as capacitor C_{sn} value is concerned, its main objective is to set the maximum voltage rate of change across the switch at turn-off. Therefore, by imposing a given maximum voltage rate of change (e.g. 1.5V/ns) and computing the maximum charge current (i.e. the magnetizing current at nominal power and minimum input voltage), it is possible to determine the value of C_{sn} .

For the selection of the inductor L_{sn} value, it is necessary to take into account both the switch current stress and the soft switching condition. A possible criterion is to limit the overcurrent due to the snubber action to the level implied by the conventional flyback topology, which poses a lower bound on the inductance value. On the other hand, the soft switching condition requires the resonance period of the snubber to be lower than the minimum switch on-time in order to allow a complete inversion of the voltage across the snubber capacitor C_{sn} . This criterion poses an upper bound to the inductance value. Other criteria, e.g. the inductor volume, could be taken into account to guide the snubber design.

B. Forward rectifier

Thanks to the presence of the reset capacitor at the secondary side, the forward rectifier can be designed to draw

current even at very low input voltage, overcoming the typical limitation of step-down topologies used as PFC's. As it has been shown in [1], the transformer can be designed as in any standard forward converter with resonant reset. The only aspect that must be carefully considered is the choice of the magnetizing inductance and the turns ratio. In particular, the latter determines the time interval, around the input voltage zero crossing, during which enough boost capability must be

provided in order to draw current from the line during the whole line period. Also the choice of the resonant capacitor value C_r strongly influences both switch voltage stress and input current waveform. As suggested in [1], it was selected so that the switch off-interval corresponding to the minimum input voltage allows one fourth of the resonance between C_r and the transformer magnetizing inductance to occur, as shown in Fig. 2a.

TABLE II
CONVERTER PARAMETERS

Forward rectifier:	$n = N_2/N_1$	0.56	
	C_{f1}	1	[μ F]
	C_{d1}	0.5	[nF]
	R_{d1}	100	[Ω]
	C_{d2}	470	[pF]
	R_{d2}	75	[Ω]
	C_r	10	[nF]
	L_F	300	[μ H]
	C_L	4400	[μ F]
Flyback rectifier:	$n = N_2/N_1$	0.165	
	C_{f1}	1	[μ F]
	C_{sn}	5	[nF]
	L_μ	1	[mH]
	L_d	15	[μ H]
	L_{sn}	300	[μ H]
	C_d	2	[nF]
	R_d	23	[Ω]
	C_L	4400	[μ F]

TABLE III
WORST CASE VOLTAGE AND CURRENT STRESSES

Forward:	U_{SWpk}	750 V	$P_o = 200$ W, $U_i = 90$ V _{RMS} , $t = 7$ ms after input voltage zero crossing.
	I_{SWpk}	7.4 A	$P_o = 200$ W, $U_i = 260$ V _{RMS} , $t = 5$ ms after input voltage zero crossing.
	U_{Dfpk}	510 V	$P_o = 200$ W, $U_i = 90$ V _{RMS} , $t = 7$ ms after input voltage zero crossing.
	U_{Drpk}	440 V	$P_o = 200$ W, $U_i = 90$ V _{RMS} , $t = 7$ ms after input voltage zero crossing.
	I_{Drpk} , I_{DFpk}	13.2 A	$P_o = 200$ W, $U_i = 260$ V _{RMS} , $t = 5$ ms after input voltage zero crossing.
Flyback:	U_{SWpk}	850 V	$P_o = 200$ W, $U_i = 260$ V _{RMS} , $t = 5$ ms after input voltage zero crossing.
	I_{SWpk}	6.84 A	$P_o = 200$ W, $U_i = 90$ V _{RMS} , $t = 5$ ms after voltage zero crossing.
	U_{Drpk}	210 V	$P_o = 200$ W, $U_i = 260$ V _{RMS} , $t = 5$ ms after input voltage zero crossing.
	I_{Drpk}	41.5 A	$P_o = 200$ W, $U_i = 90$ V _{RMS} , $t = 5$ ms after input voltage zero crossing.

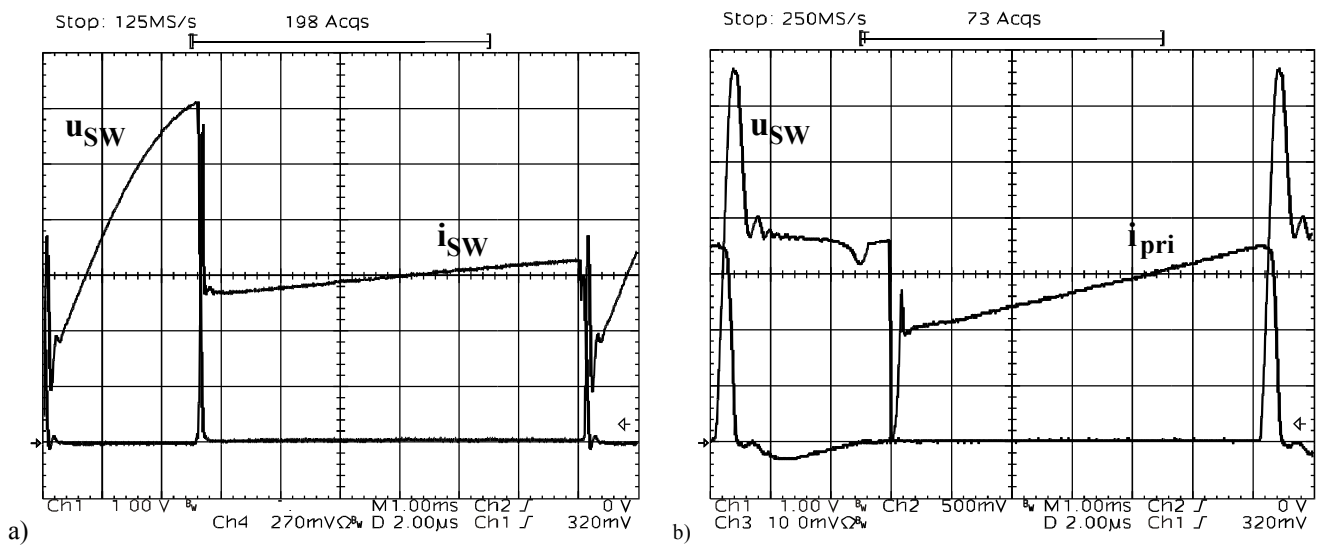


Fig. 2 - Voltage and current waveforms in a switching period at instant $t = 5$ ms from the beginning of the line half period [$u_{sw} = 100$ V/div, i_{sw} , $i_{pri} = 2$ A/div, horizontal = 2μ s/div]. a) forward rectifier; b) flyback rectifier (transformer primary current is shown)

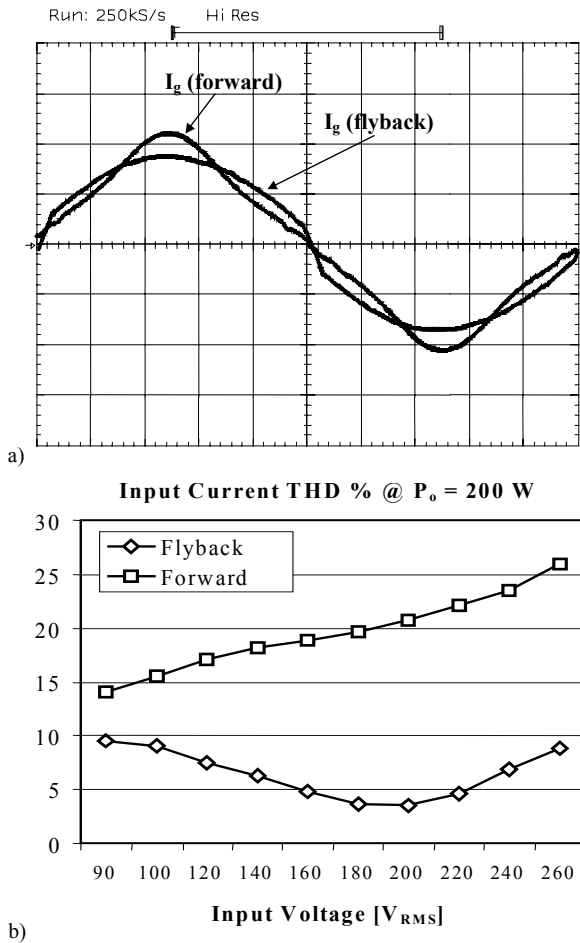


Fig. 3 - a) Comparison between filtered input current waveforms in a line period @ $U_g = 90V_{RMS}$, $P_o = 200W$ [$i_i = 2A/div$, $x = 1ms/div$]; b) Total Harmonic Distortion as a function of input voltage for nominal output power.

Following the design procedures reported in [1,2] we determined the parameter values listed in Table II.

Fig. 2 shows voltage and current waveforms of both converters taken at the input voltage peak (@ $U_i = 90 V_{RMS}$, $P_o = 200 W$) in a switching period. In particular, Fig. 2a refers to the forward converter, with the classical switch voltage waveform imposed by the resonance between the transformer magnetizing inductance and the resonant capacitor C_r (see Fig. 1a), while Fig. 2b refers to the flyback rectifier, where the high voltage peak at the switch turn-off is caused by the resonance between leakage inductance L_d and resonant capacitor C_{sn} . Note that the current waveform here shown is the transformer primary current.

The worst case switch voltage and current stresses measured on the implemented prototypes are given in Table III. It is possible to note that the high voltage stress of the flyback topology is partially due to the high transformer turns ratio, needed to achieve zero voltage switching at turn off.

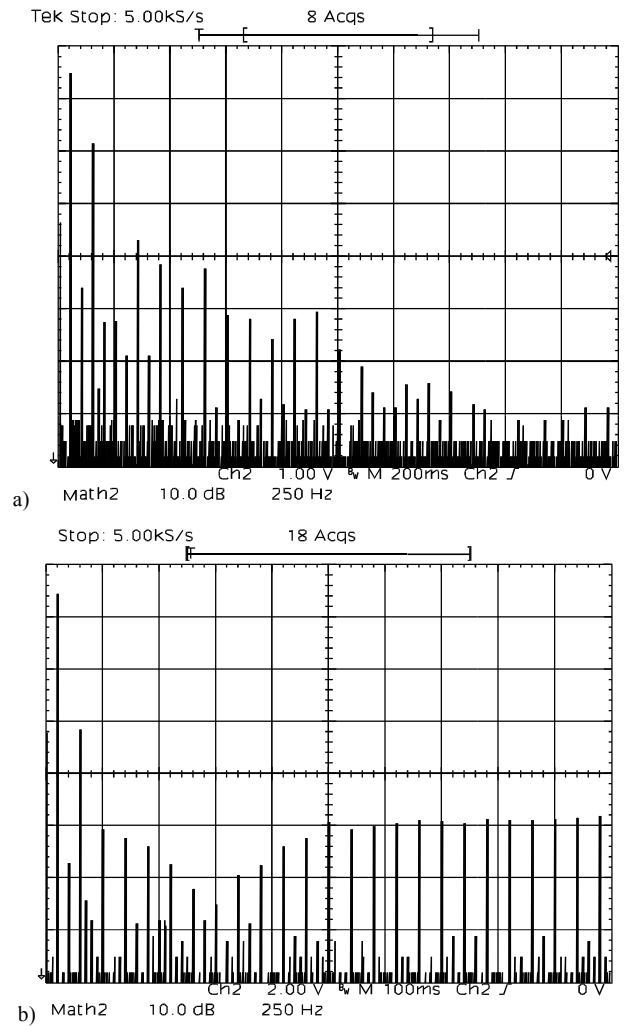
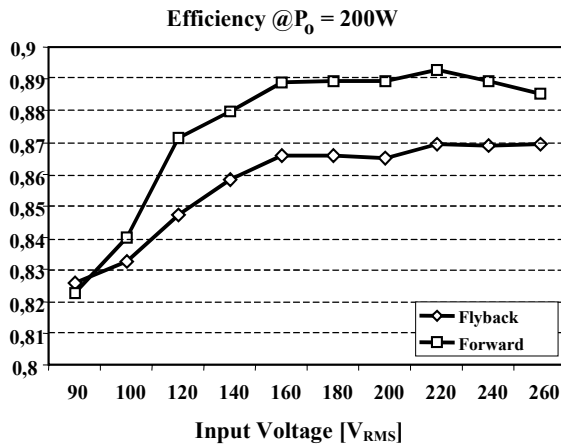


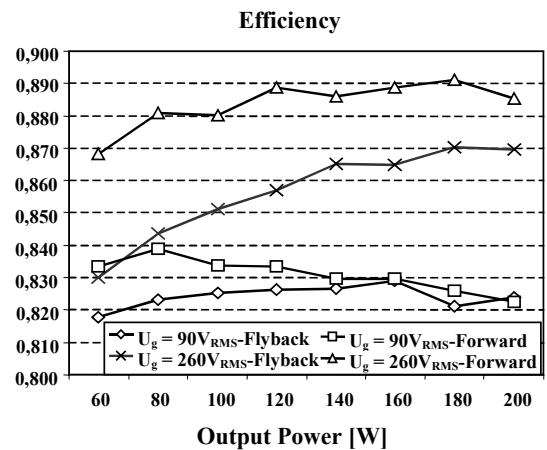
Fig. 4 - Comparison of input current harmonic spectra @ $U_g = 230V_{RMS}$, $P_o = 200W$. Top line = 5dBA, vertical scale = 10 dB/div, horizontal scale = 250 Hz/div. a) forward; b) flyback.

IV. HARMONIC CURRENT ANALYSIS

The adopted control technique is a simplification of the one proposed in [3,4] for flyback rectifiers operating in CCM, so we expected a better performance in terms of low-frequency input current harmonic content as respect to the forward rectifier. This is evident in the filtered input current waveforms shown in Fig. 3a (@ $U_g = 90 V_{RMS}$, $P_o = 200 W$), and in the total harmonic distortion curves of Fig. 3b. However, the input current spectra reported in Fig. 4 taken at $U_g = 230 V_{RMS}$ and nominal output power, shows their compliance with low frequency harmonic standards like EN61000-3-2. Note that different control techniques for the forward converter can improve its input current distortion [1].



a)



b)

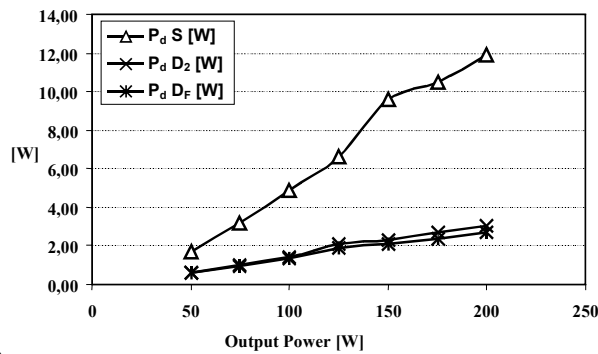
Fig. 5 - Comparison of overall efficiency as a function of: a) input voltage and b) output power.

V. CONVERTER EFFICIENCY

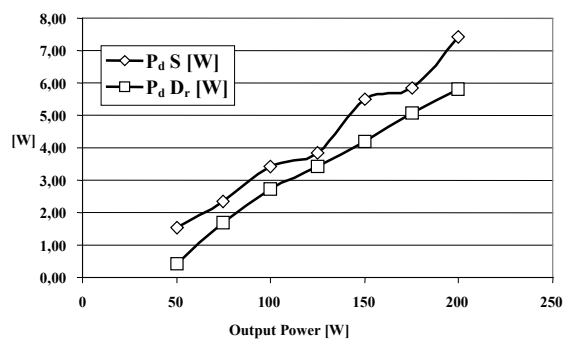
The converter overall efficiency, including the control circuit, was measured for both prototypes as a function of the input voltage @ $P_o = 200W$ and the result is shown in Fig. 5a: as we can see, the forward converter achieves a better efficiency in all the input voltage range, except at the minimum value of $90V_{RMS}$, which corresponds to maximum duty-cycle and worse reverse recovery of the freewheeling diode. As previously stated, with our design, in these conditions, the residual voltage across the resonant capacitor at the beginning of the switch on time is maximum (Fig. 2a), in order to obtain the maximum boost action. This determines an increase of the free-wheeling diode voltage stress and consequent worse reverse recovery behavior. The difference between the two converters increases at lower output power, as can be seen from Fig. 5b: the snubber action in the flyback converter re-circulates energy to the input, causing an almost constant power loss, which becomes more apparent at low output power.

To further investigate this aspect and better identify the origin of the power losses, we took into account the power

dissipation on the active devices for both the converters. To derive the power loss on each device we performed temperature measurements on the heatsinks at different output power levels. Of course, each component was given a separate and thermally isolated heatsink. Then, each device was polarized in the active region with a controlled dc current so as to get the same previously measured thermal equilibrium temperatures on the heatsink. The power measurement was finally performed multiplying the dc voltage drop and the dc current on the device. Results are shown in Fig. 6. In particular, Fig. 6a shows the achieved results for the forward converter, while Fig. 6b illustrates the results for the flyback converter. It is possible to see the much smaller power loss on the switch implied by the soft-switching operation of the flyback converter. The losses on diode D_r are instead close to those measured on the two forward diodes together. The overall efficiency of the flyback converter is therefore lower than that of the forward converter essentially because of core and copper losses on the magnetic components (transformer and passive snubber).

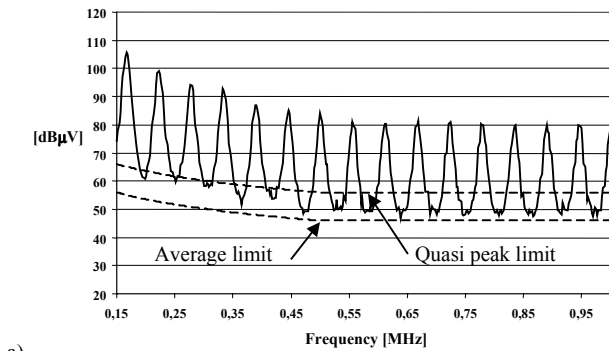


a)

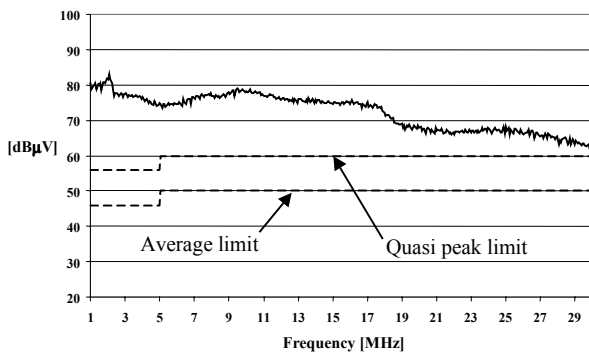


b)

Fig. 6 - Comparison of power losses on the active devices a) forward and b) flyback.



a)

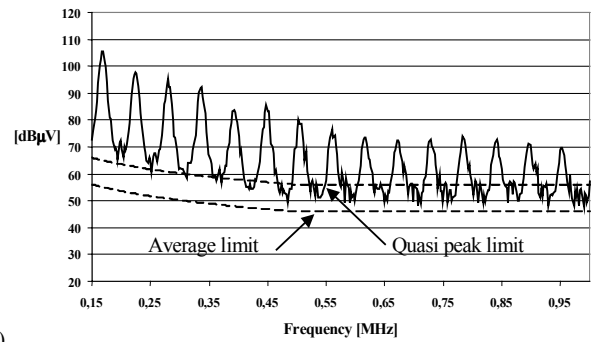


b)

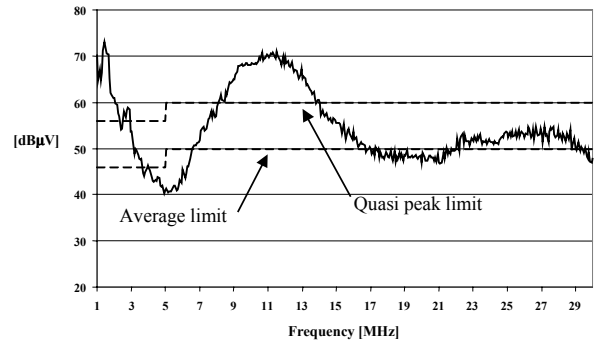
Fig. 7 - Conducted electromagnetic noise measurement for the forward rectifier.

VI. CONDUCTED EMI MEASUREMENTS

For a complete comparison between the two topologies, conducted EMI measurements were performed without any input filter, except the differential mode capacitor C_{fi} shown in Fig. 1. Fig. 7 shows the results for the forward rectifier (peak measurements). In particular Fig. 7a shows the range between 150 kHz and 1 MHz, where the noise is almost entirely differential mode, as the presence of switching frequency harmonics indicates. Fig. 7b instead shows the range between 1 MHz and 30 MHz, where a dominant common mode noise component can be observed. Average and quasi-peak limits (EN55022 Class B) are also included for comparison. The results of the same measurement on the flyback topology are shown in Fig. 8, where, again, Fig. 8a refers to the 150 kHz and 1 MHz range and Fig. 8b to the 1 MHz and 30 MHz range. Also in the flyback case, the lower frequency part of the spectrum is dominated by differential mode noise, while common mode noise seems to be largely prevailing in the higher frequency range. Comparing the two spectra, a lower noise is measured for the flyback rectifier, as it could be expected, because of its soft-switching operation. It is possible to relate this difference to the reduced dv/dt characterizing the flyback switch at turn-off, which essentially reduces common mode noise injection. This reduction is due both to the limitation of the capacitive current injected by the heatsink and to the smaller effects of the diode recovery current implied by the smaller dv/dt . The reduction of



a)



b)

Fig. 8 - Conducted electromagnetic noise measurement for the flyback rectifier.

common mode noise is probably responsible also for the slight difference in the lower frequency part of the spectrum, which appears to be significant only for frequencies above 600 kHz. As far as differential mode noise is concerned, since both converters present a chopped input current waveform, with almost the same amplitude, the measured levels are quite close, especially in the lower frequency range of the spectrum.

VII. CONCLUSIONS

An exhaustive comparison of two single-switch isolated high-quality rectifier, suitable for low power applications with universal input voltage range, is carried out in this paper. Analysis includes: main design guidelines, voltage and current rating of active devices, power dissipation of main devices, overall efficiency and EMI noise generation. The results are achieved by measurements on two 200 W fully developed prototypes. Based on these it is possible to say that the flyback converter, thanks to its soft-switching operation, is capable of offering a significant advantage in terms of EMI generation. The forward converter, anyway, is capable of a better performance in terms of efficiency and rating of the power devices.

REFERENCES

- [1] G. Spiazzi, "A High-Quality Rectifier Based on the Forward Topology with Secondary-Side Resonant Reset," Proc. of IEEE Power

- Electronics Specialists Conf. (PESC), Galway, June 2000, pp.781-786.
- [2] G. Spiazzi, S. Buso, D. Tagliavia, "A Low-Loss High-Power-Factor Flyback Rectifier Suitable for Smart Power Integration," Proc. of IEEE Power Electronics Specialists Conf. (PESC), Galway, June 2000, pp.805-810.
- [3] J. P. Gegner, C. Q. Lee, "Linear Peak Current Mode Control: A Simple Active Power Factor Correction Control Technique for Continuous Conduction Mode," PESC Conf. Proc., 1996, pp. 196-202.
- [4] Z. Lai, K. Smedley, "A Family of Power-Factor-Correction Controllers," APEC Conf. Proc., 1997, pp. 66-73.